

WILOCSIM: SIMULATION TESTBED FOR WLAN LOCATION FINGERPRINTING SYSTEMS

Chamal Sapumohotti*, Mohamad Y. Alias, and Suwei Tan

Faculty of Engineering, Multimedia University, Cyberjaya, Malaysia

Abstract—This paper introduces a novel simulation testbed for investigating WLAN indoor localization systems. This testbed referred to as *WiLocSim* consists of a novel beacon received signal strength (RSS) simulator which provides realistic modeling of beacon signal characteristics such as multipath propagation, measurement noise and body loss. Each component of the simulator is individually modeled and verified prior to integration. In addition, the capabilities of the testbed are demonstrated using two variants of the nearest neighbor classification based indoor localization algorithm. Unlike conventional measurement based performance evaluation, the proposed testbed provides a reproducible environment for accurate evaluation and analysis of indoor localization systems. More importantly, it significantly reduces the high labor cost typically required in measurement based testbed.

1. INTRODUCTION

Availability of accurate location information in indoor environments adds significant value to mobile device users. Location information enables navigation in large indoor environments as well as context aware information delivery [1]. The Global Positioning System (GPS) [2] technology has become the de-facto standard for outdoor localization. GPS requires line-of-sight (LOS) between GPS satellites and client device for accurate localization. Unfortunately, GPS is impractical for indoor applications as the direct paths between satellites and the client are obstructed when the client device is located inside buildings [1, 3, 4]. Recent proliferation of Wireless Local Area Network (WLAN) devices presents an opportunity to utilize the widely available WLAN beacon signals as distinctive fingerprints for indoor location. This method is referred to as location fingerprinting [5].

Received 8 October 2012, Accepted 9 November 2012, Scheduled 13 November 2012

* Corresponding author: Chamal Sapumohotti (chamalsm@yahoo.com).

Location fingerprinting utilizes periodic beacons broadcast by WLAN Access Point (AP) to client devices. A typical location fingerprinting implementation consists of two phases: online phase and offline phase [5]. In the offline phase, received signal strength (RSS) data collected at predefined locations (referred to as calibration points) and the corresponding location information are stored in a database (referred to as radio map). The calibration points are distributed in a uniform grid such that the spacing between adjacent calibration points is constant. Beacon RSS data is processed prior to storage in the radio map. The types of RSS data stored in the radio map depend on the localization algorithm. The simplest form is to store the summary statistics of the beacon RSS such as mean and variance, while more complex algorithms require the beacon RSS histogram or the beacon RSS probability distribution. In the online phase, the beacon RSS measured in real-time by a client device is compared to the radio map to infer its location. To date, a wide variety of algorithms have been proposed to infer the user location, such as the nearest neighbor classification [6], Bayesian filtering [5], Bayesian networks [7] and neural networks [8].

There is a plethora of design choices for designing a new indoor localization system. For examples, the number and location of calibration points, the number and location of APs to be included in the radio map, the type of beacon statistics to be stored in the radio map, the localization algorithm to be used and parameters configuration of the localization algorithm. These choices affect the deployment cost, localization accuracy, database requirement, computational complexity and the scalability of the system.

In current literature [5–9], indoor localization algorithms are typically evaluated in the following manner. First, beacon RSS at calibration points are collected and processed to create a radio map of the target area. Afterwards, RSS measurements at some predefined locations (called test points) are collected and fed into the algorithm for location prediction. The location accuracy of the algorithm is evaluated by computing the average error which is the average Euclidean distance between the location estimates and the actual locations of the test points.

A measurement based evaluation methodology cannot accurately and reliably assess an indoor localization system. Specifically, beacon RSS is affected by several random processes. First, due to multipath propagation of beacon signals, the RSS may change significantly even for locations which are very close to each other. Second, there is temporal variation in the RSS even for the same location. Consequently, a sufficiently large number of test points that are

uniformly distributed are needed to more accurately evaluate the system. However, collecting large amount of data at test points is both time consuming and labor intensive. Hence existing experimental study are typically restricted to a small number of test points. For example, existing indoor localization systems were evaluated against test points that range from 30 to 107 [5–9]. Such limitation could result in inaccurate performance estimations. In Section 4.3, a detailed discussion on the labor cost associated with test point data collection effort and the accuracy of subsequent performance estimation is given.

Simulation has been proven to be invaluable for the development and testing of wireless technology applications [24]. It provides in-depth execution details, a rapid prototyping environment, nonintrusive debugging, and repeatability while removing the high labor cost associated with measurement studies [25]. Testbed is an environment which supports data collection for the purpose of evaluating a system. This includes the ability to control environment parameters and scenarios. A testbed provides metrics for evaluation and allows the experimenter a fine-grained control over test parameters [24, 25]. In this paper, WiLocSim is presented as a simulation testbed which combines the advantages of simulation and testbed environment. It facilitates the design and accurate assessment of location fingerprinting based indoor localization systems. The designer of location fingerprinting systems has a wide array of algorithms to choose from and a variety of operating environments to deal with. This testbed serves as a tool to evaluate these design options and trade-offs under different assumptions and scenarios. For instance, WiLocSim can provide comprehensive methods for evaluating algorithms, generation of performance indicators, study of algorithm trade-offs. To the best of our knowledge, this is the first simulation testbed presented for WLAN location fingerprinting systems. At present, the testbed supports IEEE 802.11g WLAN technology [10] as it is widely used by existing mobile devices. The core of the testbed is a WLAN beacon RSS simulator, which consists of detailed WLAN beacon generation process and various modules (multipath propagation, body loss and measurement noise) that affect the beacon RSS.

The rest of this paper is organized as follows. In Section 2, the beacon RSS generation models are described in detail. The proposed simulation testbed is presented in Section 3. In Section 4, the capabilities of the testbed are demonstrated using two variants of the nearest neighbor classification based indoor localization algorithm. Section 5 presents some concluding remarks.

2. PHYSICAL PROCESS MODELS FOR BEACON RSS SIMULATOR

The most important component of the proposed simulation testbed is the beacon RSS simulator. There are three main sources which impact beacon RSS: (i) radio wave propagation characteristics of the environment, (ii) temporal changes in RSS due measurement noise and (iii) loss of signal strength due to obstruction by the user. The proposed beacon RSS simulator models all three sources to provide a good approximation of RSS behavior in real-world environments. These three models are presented in this section. The overall RSS simulator will be presented in Section 3.

2.1. Multipath Propagation Model

A WLAN AP broadcasts periodic beacon frames to advertise its availability and operating parameters. For instance, typical deployment uses a period of 100 ms [16]. In addition, start of the beacon frame includes two preambles, referred to as short preamble and long preamble. The short preamble is used for frequency and timing synchronization and the long preamble is used for computing the beacon RSS [17]. Since IEEE 802.11g uses OFDM modulation with 64 subcarriers the frequency domain representation of the long preamble is given as

$$LP(f) = \{0, 0, 0, 0, 0, 0, 1, 1, -1, -1, 1, 1, -1, 1, -1, 1, 1, 1, 1, 1, 1, -1, -1, 1, 1, -1, 1, -1, 1, 1, 1, 0, 1, -1, -1, 1, 1, -1, 1, -1, 1, -1, -1, -1, -1, -1, 1, 1, -1, -1, 1, -1, 1, 1, 1, 0, 0, 0, 0, 0\} \quad (1)$$

This frequency domain representation is converted to time domain representation, $LP(t)$ by performing Inverse Fast Fourier Transform (IFFT) of length 64 on $LP(f)$ and adding a cyclic prefix which is 1/4 of the IFFT sequence. This time domain signal is then modulated using the carrier frequency. The transmit OFDM signal of the long preamble is given as

$$S_0(t) = I(t) + jQ(t) \quad (2)$$

where $I(t)$ is the in-phase signal and $Q(t)$ the quadrature signal. If only a single copy of the transmit signal is received at the transmitter, the RSS calculation would be straightforward. However, due to multipath propagation, multiple copies of the signal at different power levels are received at different times.

Multipath propagation refers to the phenomenon that results in radio signals arriving at the receiver via multiple propagation paths. The paths could consist of the direct path, reflected paths,

diffracted paths and scattered paths. In an indoor environment, ray tracing techniques [11–14] can be used to derive each of the multipath components. The received power in dBm of the i th path which arrives at the receiver can be expressed as [11]

$$P_i = P_{ap} + G_{ti} + G_{ri} - \left(PL_i + \sum L_i \right) \quad (3)$$

where, P_{ap} is the transmit power of the AP in dBm, G_{ti} represents the transmitter antenna gain at the departure angle of the path, G_{ri} represents the receiver antenna gain in the direction of arrival of the path, PL_i is the distance dependent path loss and L_i represents the losses at dielectric boundaries (e.g., reflection loss and transmission loss). The path loss in dB is given by,

$$PL_i = 32.4 + 20 \log_{10}(f_c) + 20 \log_{10} \left(\frac{r_i}{1000} \right) \quad (4)$$

where, the path loss is given by the free space path loss for a distance equal to the total length of the i th path r_i given in meters [15]. The carrier frequency f_c is in MHz, and for 802.11g it is around 2.4 GHz. For precise representation, the operating channel of the WLAN is required. For example, channel 1 has a center frequency of 2.412 GHz with a channel separation of 5 MHz. The multipath power in dBm can be expressed as

$$P_{mp} = P_1 + 10 \log_{10}(P_r) \quad (5)$$

where, P_1 is the signal power in the first arrived multipath signal and P_r the relative power ratio defined as

$$P_r = \frac{p_{mp}}{p_1} \quad (6)$$

In Equation (6), p_{mp} and p_1 are the average power of the multipath signal in watt and power of the first arrived path in watt, respectively. p_1 is given by

$$p_1 = \frac{1}{K} \int_{t=t_{cp}}^{t_s} |S_1(t)|^2 dt \quad (7)$$

where, K is a constant which depends on the antenna and the OFDM symbol time. The OFDM symbol time is given by t_s and the cyclic prefix length in time given by t_{cp} . S_1 is the first arrived multipath signal and can be expressed as

$$S_1(t) = V_1 [S_0(t)] \quad (8)$$

where, V_1 is the voltage amplitude of the first received multipath signal. More generally the i th signal path can be written as

$$S_i(t) = V_i [S_0(t - \tau_i)] \quad (9)$$

where, V_i is the voltage amplitude of the i th received multipath signal. Time delay of the path relative to the first arrived path τ_i is given as

$$\tau_i = \frac{r_i - r_1}{c} \quad (10)$$

where, r_1 is the length of the first arrived multipath signal and c is the speed of light.

Now, p_{mp} , which is the average power of the multipath signal in watt, can be expressed as

$$p_{mp} = \frac{1}{K} \int_{t=t_{cp}}^{t_s} \left| \sum_{i=1}^n S_i(t - \tau_i) \right|^2 dt \quad (11)$$

where, n is the number of significant multipath.

Using the expressions for p_{mp} and p_1 , the relative power ratio can be expressed as

$$P_r = \frac{\sum_{t=t_{cp}}^{t_s} \left| \sum_{i=1}^n \alpha_i S_0(t - \tau_i) \right|^2}{\sum_{t=t_{cp}}^{t_s} |S_0(t)|^2} \quad (12)$$

Here the integrations have been replaced by summations and the normalized voltage factor α_i is defined as

$$\alpha_i = \frac{V_i}{V_1} \quad (13)$$

Alternatively, α_i can be indirectly calculated by considering the power of each path as

$$\alpha_i = \sqrt{10^{(RP_i)/10}} \quad (14)$$

where, the relative power of the i th path RP_i is given by

$$RP_i = P_i - P_1 \quad (15)$$

2.2. Body Loss Model

Human body creates signal attenuation at 2.4 GHz, which is the operating frequency of IEEE 802.11g system. This user induced loss is referred to as body loss and it has two main contributing factors. First, the user grip adds a constant loss provided that the grip and the orientation of the device are kept constant. Second, if the line-of-sight (LOS) between the AP and the device is obstructed by the body, there is additional loss. The body loss parameters depends on the device used and the user grip [18]. For this research, the body loss parameters were estimated from experiment using an LG optimus1 P500 mobile device. The impact of user on RSS was studied with the client and AP 10 m apart for the following cases:

- (i) No user present.
- (ii) The user is holding the device and the device is in LOS with the AP.
- (iii) The user is holding the device and the LOS between the device and the AP is obstructed by user body.

From the results, it was shown that the first case had the highest average RSS while the second case had a signal strength loss of 4 dB on average. On the other hand, the third case reported an average signal strength loss of 10 dB from no user present case. From the experimental results, the body loss (hand grip) is simulated by adding a constant loss of 4 dB to the multipath RSS calculated using the multipath model. If the direct path between the AP and device is obstructed by the user, an additional 6 dB is added.

2.3. Measurement Noise Model

A situation when the propagation environment and client position is constant is referred to as a static environment. The measurement noise is defined as the temporal change of RSS in a static environment. The main contributors of measurement noise at the AP side are Inphase-Quadrature (IQ) imbalances, carrier phase noise, spurious signals and transients, and nonlinearities in the amplifiers [19]. On the client side, synchronization errors add random noise to the beacon RSS readings which are mainly contributed by timing errors and frequency errors [17]. An empirical approach to model the measurement noise was used because the physical processes which contribute to measurement noise and the parameters of these processes are too complex to be modeled deterministically. Therefore a model based on measurement data has been proposed and verified to be reasonably accurate by comparing the cumulative distribution function (CDF) of the data generated by the measurement noise model with the CDF of experimental data.

In order to isolate effects of beacon measurement noise, it is necessary to have a static environment to eliminate external interference at 2.4 GHz from sources such as other wireless APs and microwave ovens. Hence, the experiment was conducted in Multimedia University anechoic chamber (see Figure 1) which is able to operate in the frequency range from 30 MHz to 18 GHz [20]. An anechoic chamber is able to remove multipath propagation and unwanted interference from any outside signal sources. A Cisco WAG160N wireless router operating in 802.11g mode and a TP-Link TL-WR340G wireless router were used as APs. Also, an LG optimus1 P500 Android phone and a



Figure 1. Experiment setup inside anechoic chamber.

Table 1. Experiment description.

Experiment ID	Active AP	Client Device	Objective
Experiment 1	Cisco	Phone	Impacts of received signal strength
Experiment 2	TP-Link	Phone	Impacts of AP type
Experiment 3	Cisco, TP-Link	Phone	Impacts of co-channel interference
Experiment 4	Cisco	Laptop	Impacts of client device

Dell laptop with Intel wireless 3945G card were used as client devices for the experiment.

The experiment was designed to investigate the effects of device dependency, received power and co-channel interference on measurement noise. The received power was controlled indirectly by varying the distance between the AP and the client device. The two APs were placed at a distance separation of 6 m. The client device is placed between the APs, and the beacon measurements are recorded at 1 m increments for distance from 1 m to 5 m from the APs. 150 beacons were captured by client device for each point in all experiments. More details of the experiment can be found in our previous work [21]. Altogether, four experiments were conducted to investigate the behavior of measurement noise. Each experiment utilized a different combination of AP and client devices. The description for each experiment is given in Table 1.

From our previous analysis of the collected data, it was found that the measurement variance is very high when the distance between

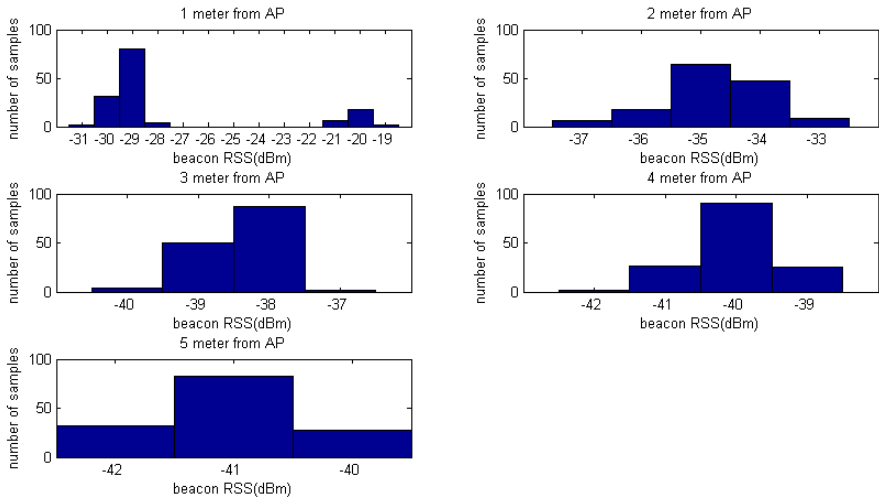


Figure 2. Sample beacon RSS histograms from experiment 1.

the AP and the client device is 1m due to the high power level. The measurement variance drops to a value in the range of 2 dB when the distance is greater than or equal to 2 m. The set of histograms for all 4 experiments have similar characteristics and the sample histogram set for Experiment 1 is presented in Figure 2. From the figure, it is evident that the beacon histogram at 1 m distance is significantly different from histograms at other distances due to RSS readings which are spread over a larger range (−19 dBm to −31 dBm). When the distance is increased, the histograms have a much narrower range and can be approximated by a normal distribution. The model for measurement noise is developed based on these observations.

2.3.1. Proposed Measurement Noise Model

The suggested model is derived from a normal distribution, where the mean and variance of the model is equal to the sample mean and variance, respectively. The RSS is a discrete value. In order to obtain the discrete RSS, the value generated from the continuous normal distribution is rounded to the nearest integer. The probability of obtaining a beacon RSS reading X equal to X_i is given as

$$P(X = X_i) = \int_{X_i-0.5}^{X_i+0.5} N(X)d \tag{16}$$

where, the function $N(X)$ is a normal distribution with mean and variance given by \bar{x} (sample mean) and s (sample standard deviation). $N(X)$ is expressed as

$$N(X) = \frac{1}{\sigma\sqrt{2\pi}} e^{-0.5\left(\frac{X-\bar{x}}{s}\right)^2} \quad (17)$$

2.3.2. Measurement Noise Model Verification

The accuracy of the proposed model for modeling measurement noise is verified by comparing the CDF of the data generated by the proposed model with the CDF of the measurement data. A graphical plot of the distributions [22] is used for this purpose. If the CDFs are similar, then the model can be implied to be accurate. All the plots showed that the proposed model is a good approximation for measurement noise for distance above 1 m. A sample plot is shown in Figure 3. In the figure, the $y = x$ line (solid black line) indicates a high similarity between the proposed model and the measurement data for all cases except for 1 m separation. At 1 m separation, a significant deviation from normal distribution was observed in the beacon histograms. This abnormal behavior could be due to the receiver front end saturation as a result of high power levels observed when the distance between AP and client is only 1 m. For the simulation of measurement noise, the sample average is calculated by the multipath model and the body loss model. From our previous work [21], it was found that a 2 dB variance is a good approximation for measurement noise. Thus, a 2 dB variance is used in the simulation testbed.

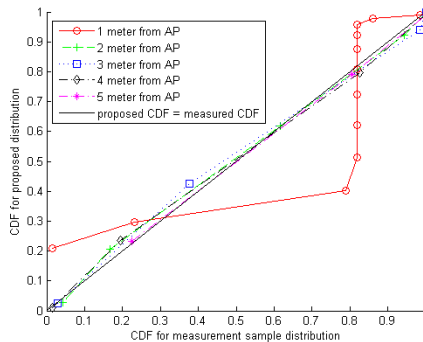


Figure 3. Experiment 2 Q-Q plot, proposed distribution vs. measured distribution.

3. SIMULATION TESTBED

3.1. Beacon RSS Simulator

The beacon RSS Simulator as shown in Figure 4 serves as the core of the testbed. The RSS Simulator integrates the three models discussed in Section 2 to simulate beacon RSS. Scenario information and client location are required as inputs to the multipath model. Scenario information includes the description of the environment used by the ray tracer, location as well as the properties of AP and client radio. The multipath model calculates the multipath RSS as described in Section 2.1. The output of the multipath model is the multipath RSS;

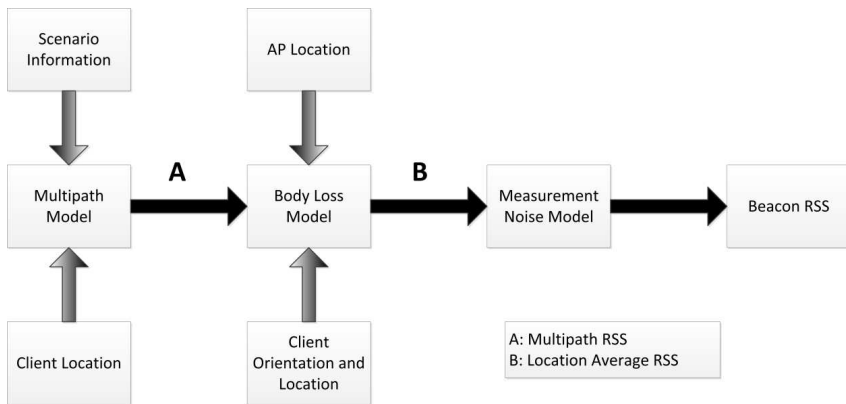


Figure 4. Beacon RSS Simulator.

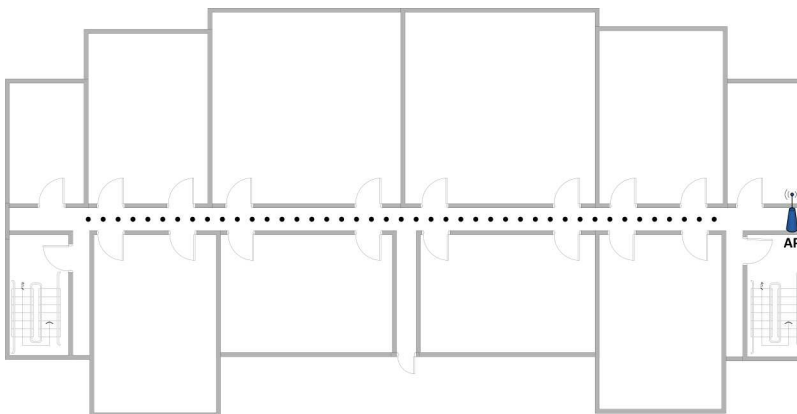


Figure 5. Measurement setup.

this output is fed into the body loss model. The body loss model considers the location of the AP as well as the location and orientation of the user. Next the body loss value is calculated as described in Section 2.2 and it is added to the multipath RSS. The output of the body loss model is the location average RSS. This output is fed into the measurement noise model which creates temporal variation in the beacon RSS. Measurement noise model adds measurement noise according to Section 2.3 and outputs the final result which is the beacon RSS.

A simple scenario was used to verify the applicability of the simulator in generating RSS data. A measurement experiment was conducted in wing A of the first floor of Faculty of Engineering in Multimedia University (MMU), Malaysia (see Figure 5). An AP was placed at the right end of the corridor. The corridor is 1.8m in width and 2.5m in height. The AP used has a transmit power of 17 dBm. Measurements were collected at test points starting 5 m away from the AP until 56 m. Test points were located every 0.6 m in the measurement path and the path is shown in the figure by the dotted line. At each point, 60 samples were collected.

In order to verify the accuracy of the beacon RSS simulator, a simulation experiment was conducted using identical setting as in the measurement experiment. A simple ray tracer was utilized for calculating the power of reflected waves. Only the first order reflections from the four walls, ceiling and the floor were considered. In order to simplify the calculations and since the exact electromagnetic parameters of the walls were not available to calculate Fresnel reflection coefficients, a fixed reflection loss is added to each of the reflections.

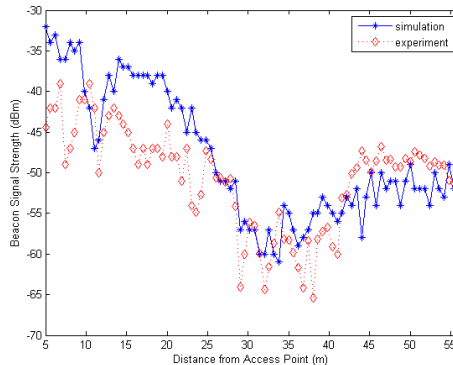


Figure 6. Comparison between simulation and experiment data.

Several rounds of simulations with different reflection loss values were conducted and the reflection loss of 3 dB gives the best similarity to measurement data. This value of 3 dB reflection loss is used in subsequent simulations as well. The antennas are assumed to be dipole antennas. The average RSS of simulation and measurement are given in Figure 6. From the experiment, RMS error is 5.6 dB and the mean error is 2.4 dB. Thus, the simulated beacon RSS is a reasonable approximation.

3.2. Integration of the RSS Simulator into the Testbed

Figure 7 summarizes the overall simulation testbed which can be used to compare the performance of different types of radio map construction strategies and localization algorithms for different environments. Initially the locations of calibration points are calculated such that the calibration points are distributed uniformly in the area for which localization is performed. The resolution of the calibration points which is the distance separation between adjacent calibration points and the number of samples which are collected at each calibration point are configurable parameters. Next the calibration point RSS samples are simulated using the beacon

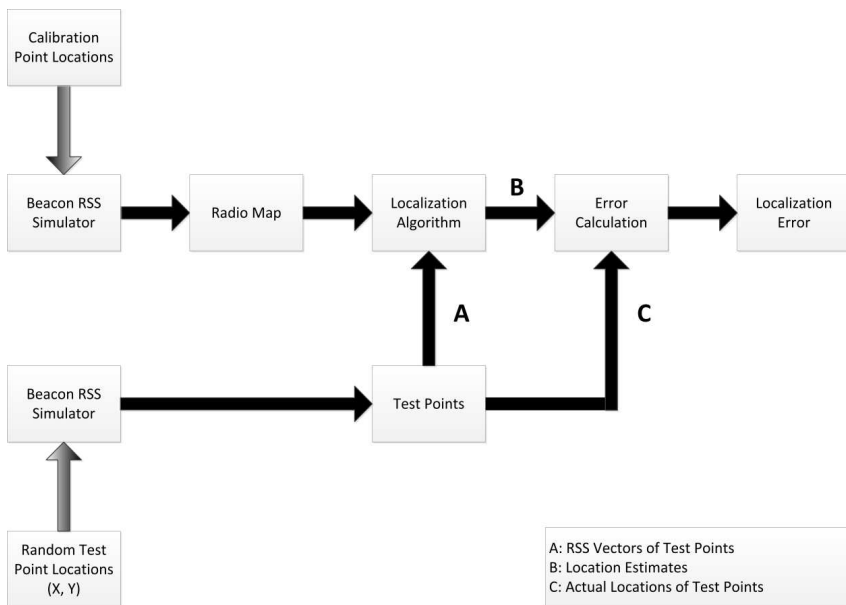


Figure 7. Simulation testbed.

RSS simulator and the radio map is constructed. The radio map construction depends on the algorithm used for localization. A summary statistic such as the mean of the sample is stored in the radio map for deterministic localization techniques such as nearest neighbor classification. For probabilistic localization techniques, the histogram of the probability distribution of the RSS for each calibration point is stored in the radio map.

The test points are used to evaluate the performance of the indoor localization system which is created by the combination of the radio map and the localization algorithm. Test points should be distributed uniformly throughout the area in which the location system operates. This is achieved by using two uniform random variables which generate x and y coordinates for the test points. The location estimates for the test points are compared with the actual location of the test points to compute the localization error. The average error of all the test points can be used to compare the performance of different indoor localization systems.

4. SIMULATOR DEMONSTRATION

This section demonstrates the capabilities of the simulation testbed by analyzing the performance of two variants of nearest neighbor (NN) classification based indoor localization algorithms: K -nearest Neighbor (KNN) and Weighted K -nearest Neighbor (WKNN). In literature, both KNN and WKNN are expected to perform better than NN for small K where K is the number of neighbors. The optimal K reported in literature [5, 23] is 3 or 4 and the location error of WKNN is expected to be less than KNN. Simulation testbed allows us to simulate large number of test points which is impractical through measurements. The error performance of the algorithm is analyzed for different number of test points. The possibility of coming up with wrong conclusions if the number of test points is not statistically significant is shown.

4.1. Nearest Neighbor Classification

The structure of a radio map designed for NN classification consists of a set of location labels for calibration points and a set of fingerprints which are collected at those calibration points. A fingerprint is represented by a vector with each dimension representing averaged beacon received RSS from an AP. The set of locations of calibration points are given by $P = \{p_1, p_2, \dots, p_n\}$, where $p_i = (x_i, y_i)$ is the x and y coordinates of the calibration point. The set of fingerprints is given by $F = \{f_1, f_2, \dots, f_n\}$. For a radio map with M access points,

A fingerprint $f_i = \langle \overline{a_{i1}}, \overline{a_{i2}}, \dots, \overline{a_{iM}} \rangle$ where $\overline{a_{ij}}$ is the averaged beacon RSS for the j th AP for i th fingerprint. If N samples are collected at each calibration point, the $\overline{a_{ij}}$ is represented as

$$\overline{a_{ij}} = \frac{1}{N} \sum_{t=1}^N a_{ij}^t \quad (18)$$

In the localization phase, the vector distance between the beacon RSS vector and all the calibration points in the radio map is computed. The vector distance between the i th calibration point and the test point is given as

$$dist(f_i, O_t) = \|f_i - O_t\| \quad (19)$$

There are many different methods to calculate the vector distance. For this simulation, Manhattan norm was used [5]. For NN the location of the calibration point which has the lowest distance to test point is the location estimate of the user.

For KNN, the geometric center of the closest K calibration points in signal space is the location estimate \hat{p} given by

$$\hat{p} = \frac{1}{N} \sum_{l=1}^K P_l \quad (20)$$

For WKNN, a weight w_{ti} is assigned to each of the K nearest calibration points in signal space which is inversely proportional to the signal space distance. The weight is given by

$$w_{ti} = \frac{1}{dist(f_i, O_t)} \quad (21)$$

If the subset of F which has the fingerprints with the largest K weights is L , a normalization factor, W_N is calculated by

$$W_N = \sum_{l=1}^K W_l \quad (22)$$

On the other hand, the location estimation for WKNN is given by

$$\hat{p} = \frac{1}{W_N} \sum_{l=1}^K W_l P_l \quad (23)$$

4.2. Simulation Setup

The simulation scenario is shown in Figure 8. In this scenario, 4 APs are located inside a hall with 30 m \times 50 m dimensions which is similar

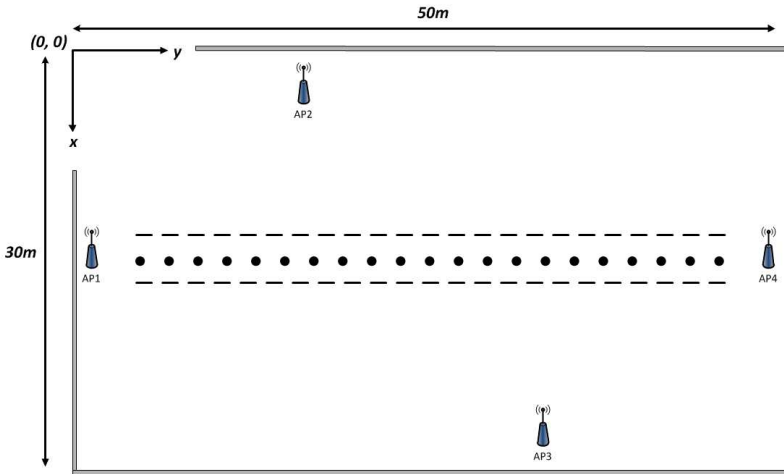


Figure 8. Simulation scenario.

to the measurement based testbed found in literature. For example, HORUS [9] used a testbed of size $26\text{ m} \times 68\text{ m}$ and RADAR [6] used a testbed of size $23\text{ m} \times 44\text{ m}$. The number of APs (four APs) was also chosen to be similar to the values used in literature. For instance, RADAR utilized 3 APs while 5 APs were used in [23]. The locations of the APs were chosen such that it creates significant variation of RSS as the user moves from one end of the corridor to the other end. The AP power level was chosen to be 17 dBm, which is the power level of the Cisco AP that was used in measurement noise experiment. Simulations assume dipole antennas at both the APs and at the client device since it is a common antenna pattern in WLAN APs and also because of its simplicity.

By using the coordinate system shown in Figure 8, the locations of the APs are as follows: AP1 (15, 1), AP2 (1, 12), AP3 (29, 38), and AP4 (15, 49), the locations of the AP were chosen arbitrarily. The calibration points for the radio map are located on the dotted line. The calibration points start from (15, 2) and end at (15, 48), while the distance separation between adjacent calibration points is 1 m. The test points are located randomly in the area between the two dashed lines. The top line is given by $x = 14$ and the bottom line is given by $x = 16$. Each calibration point is the mean of 60 samples. The test point locations were uniformly distributed throughout the localization area. The RSS for each AP at each test point is simulated and is used to infer the user location using the radio map. The error

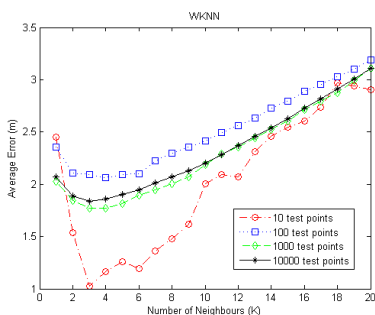


Figure 9. Average Error vs. K for WKNN.

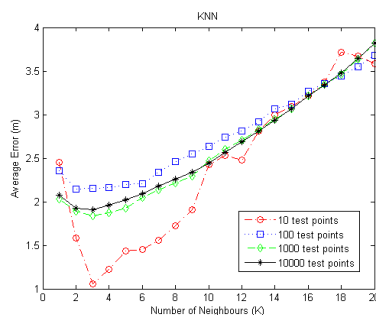


Figure 10. Average Error vs. K for KNN.

is calculated by taking the difference between the location estimation and the actual location of the test point. To illustrate the concept of requiring statistical significance in the results, the number of random locations generated is considered for 10, 100, 1000, and 10000 test points.

4.3. Results and Discussion

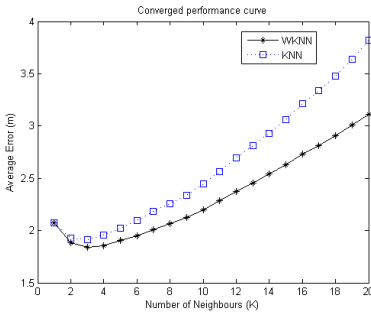
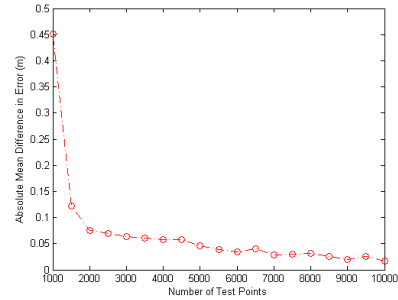
Figure 9 depicts the average error performance for WKNN algorithm, Figure 10 shows the average error performance of KNN algorithm, and Figure 11 displays the error performance of KNN and WKNN when 10000 test points are used for evaluating the performance. From the simulations, for 10 and 100 test points, it is difficult to come to a conclusion about the impact of K for the performance of KNN and WKNN. However, for 1000 and 10000 iterations the average error curve converges. From Figure 11 it can be concluded that the optimal K for both KNN and WKNN is 3. The performance degrades as the K is increased further and the performance of WKNN is slightly better than KNN. The performance of NN algorithm can be obtained from both curves by assigning $K = 1$. Both WKNN and KNN performance is better than NN for small K . Overall, the simulation results are consistent with the results found in literature [5, 23].

4.3.1. The Cost of Actually Measuring the Test Points Rather Than Simulating

The reason for not using a large number of test points in measurement based testbed is because of the high labor cost. Assume that it takes 30seconds to collect data at each test point. This duration could be

Table 2. Data collection effort.

Number of test points	Data Collection time (minutes)
10	5
100	50
1000	500
10000	5000

**Figure 11.** Performance comparison of WKNN and KNN.**Figure 12.** Convergence analysis.

much longer if the measurements are not taken in a grid. Table 2 indicates the amount of time it would have taken for data collection for each experiment. From the table, the data collection for large number of test points which could add statistical significance to the results is very tedious.

In comparison, there are costs associated with simulation setup. For instance, there is labor cost incurred for obtaining body loss parameters for a specific device and also for deriving reflection coefficient for a specific environment. However, once these parameters are determined, many different scenarios (different number of APs, different number of calibration points, etc.) can be tested without additional labor cost. If measurement based approach is utilized, each different scenario would require measurements and repeat of data collection effort.

4.3.2. Convergence of the Error Curve as the Number of Test Points is Increased

From Figures 9 and 10, it is observed that the average error curves tend to converge to the absolute average error of the indoor localization

system. An understanding of the minimum number of test points for convergence would help to reduce the computational steps. On the other hand, it is difficult to come up with a generic value as the number of optimal test points as it depends on the dimension of the environment. Therefore, monitoring of the differences between average error curves as the number of test points is increased is proposed as a solution for determining the convergence. In this approach a fixed number of test points are added in to the current pool of test points at each step. The convergence metric is calculated for the current number of test points by getting the mean absolute difference between the average error curve for current pool of test points and error curve for previous pool prior to the addition of new test points. Figure 12 gives the convergence metric for calculating WKNN as the number of test point increase. In this simulation, 500 new test points were added to the test point pool at each step. The graph shows mean absolute difference between the average error curves for current pool of test points and previous pool of test points. For instance, in the graph, the mean absolute difference when the number of test points is 2000 represents the mean absolute difference between the average error curve for the 2000 test points and average error curve for 1500 test points. From Figure 12, it is observed that graphs have sufficiently converged at 2000 test points although there is a small improvement in convergence as the number of test points is increased to 10000.

5. CONCLUSION AND FUTURE WORK

Existing measurement based indoor localization system evaluation is limited due to the high labor cost involved. In fact, it requires data collection at large number of test points in order to provide a statistically meaningful assessment. In comparison, simulation offers a reliable and low cost alternative. To address this need, this paper proposed a simulation testbed for evaluating the algorithm performance in IEEE 802.11g based indoor localization systems.

This testbed referred to as *WiLocSim* was built around a beacon RSS simulator which models the main sources that affect the signal strength, i.e., multipath propagation, body loss and measurement noise. In addition, the capabilities of the simulator were demonstrated by analyzing the established results regarding nearest neighbor classification based localization algorithms. There are multiple potential applications for *WiLocSim*. For instance, this can be used by system designers to select optimal localization algorithms, algorithm parameters and radio map design strategies for a given scenario. Furthermore, researchers can also use the testbed to

benchmark new algorithms. In addition, the availability of a simulation testbed can significantly enhance the coherence of results published in the field of WLAN based indoor localization. This can be achieved by coming up with a set of benchmark deployment environments and evaluating the localization algorithm performance for these benchmark environments.

The Ray Tracer that was used with WiLocSim for these simulations is limited to rectangular areas. Thus, we had to limit our studies to corridor environments as navigation in corridors is a very important aspect in WLAN indoor localization. An obvious future work is to include a more powerful ray tracer in WiLocSim so that more complex scenarios can be studied.

ACKNOWLEDGMENT

The authors would like to thank Ministry of Higher Education (MOHE), Malaysia for supporting this work.

REFERENCES

1. Zeimpekis, V., G. M. Giaglis, and G. Lekakos, "A taxonomy of indoor and outdoor positioning techniques for mobile location services," *Journal of ACM Special Interest Group on Electronic Commerce*, Vol. 3, 19–27, 2002.
2. Engee, P. K., "The global positioning system: Signals, measurements and performance," *Int. J. Wireless Inf. Netw.*, Vol. 1, No. 2, 83–105, 1994.
3. Hightower, J. and G. Borriello, "Location systems for ubiquitous computing," *IEEE Computer Mag.*, Vol. 34, No. 8, 57–66, 2001.
4. Alsindi, N., X. Li, and K. Pahlavan, "Performance of TOA estimation algorithms in different indoor multipath conditions," *2004 IEEE Wireless Communications and Networking Conference, WCNC*, Vol. 1, 495–500, Mar. 21–25, 2004.
5. Honkavirta, V., T. Perala, S. Ali-Loytty, and R. Piche, "A comparative survey of WLAN location fingerprinting methods," *6th Workshop on Positioning, Navigation and Communication, WPNC 2009*, 243–251, Mar. 19–19, 2009.
6. Bahl, P. and V. N. Padmanabhan, "RADAR: An in-building RF-based user location and tracking system," *Proc. IEEE Conf. Comput. Commun.*, 775–784, 2000.
7. Al-Ahmadi, A. S. M., A. I. A. Omer, M. R. B. Kamarudin, and A. R. B. Tharek, "Multi-floor indoor positioning system

- using Bayesian graphical models,” *Progress In Electromagnetics Research B*, Vol. 25, 241–259, 2010.
8. Laoudias, C., D. G. Eliades, P. Kemppi, C. G. Panayiotou, and M. M. Polycarpou, “Indoor localization using neural networks with location fingerprints,” *Proceedings of the 19th International Conference on Artificial Neural Networks: Part II (ICANN’ 09)*, 954–963, Cesare Alippi, Marios Polycarpou, Christos Panayiotou, and Georgios Ellinas, Eds., Springer-Verlag, Berlin, Heidelberg, 2009.
 9. Youssef, M. and A. Agrawala. “The horus WLAN location determination system,” *Proc. of ACM/USENIX Mobisys*, Seattle, WA, Jun. 2005.
 10. IEEE WLAN standard, IEEE 802.11-2007, <http://standards.ieee.org/getieee802/download/802.11-2007.pdf>.
 11. Valenzuela, R., “A ray tracing approach to predicting indoor wireless transmission,” *43rd IEEE Vehicular Technology Conference*, 214–218, May 18–20, 1993.
 12. Athanasiadou, G. E., A. R. Nix, and J. P. McGeehan, “A ray tracing algorithm for microcellular and indoor propagation modelling,” *IEE Conf. Pub.*, v2-231, 1995.
 13. Reza, A. W., M. S. Sarker, and K. Dimyati, “A novel integrated mathematical approach of ray-tracing and genetic algorithm for optimizing indoor wireless coverage,” *Progress In Electromagnetics Research*, Vol. 110, 147–162, 2010.
 14. Haarscher, A., P. De Doncker, and D. Lautru, “Uncertainty propagation and sensitivity analysis in ray-tracing simulations,” *Progress In Electromagnetics Research M*, Vol. 21, 149–161, 2011.
 15. Rappaport, T. S., *Wireless Communications Principles and Practice*, 169–177, IEEE Press, New York, 1996.
 16. Petersen, S. and S. Carlsen, “Performance evaluation of WirelessHART for factory automation,” *IEEE Conference on Emerging Technologies & Factory Automation, ETFA 2009*, 1–9, Sep. 22–25, 2009.
 17. Heiskala, J. and J. Terry, *OFDM Wireless LANs: A Theoretical and Practical Guide*, SAMS Publishing, 2002.
 18. Rosa, F. D., X. Li, J. Nurmi, M. Pelosi, C. Laoudias, and A. Terrezza, “Hand-grip and body-loss impact on RSS measurements for localization of mass market devices,” *2011 International Conference on Localization and GNSS (ICL-GNSS)*, 58–63, Jun. 29–30, 2011.
 19. Olgaard, C., “Using advanced signal analysis to identify sources

- of WLAN transmitter degradations,” www.rfdesign.com, 2004.
20. Chung, B. K. and H. T. Chuah, “Design and construction of a multipurpose wideband anechoic chamber,” *IEEE Antennas and Propagation Magazine*, Vol. 45, No. 6, 41–47, Dec. 2003.
 21. Sapumohotti, C., M. Y. Alias, and S. W. Tan, “Effects of multipath propagation and measurement noise in IEEE 802.11g WLAN beacon for indoor localization,” *PIERS Proceedings*, 447–451, Kuala Lumpur, Malaysia, Mar. 27–30, 2012.
 22. WILK, M. B. and R. Gnanadesikan, “Probability plotting methods for the analysis of data,” Vol. 55, No. 1, 1–17, *Biometrika*, 1968.
 23. Li, B., J. Salter, A. G. Dempster, and C. Rizos, “Indoor positioning techniques based on wireless LAN,” Tech. Rep., School of Surveying and Spatial Information Systems, UNSW, Sydney, Australia, 2006.
 24. Tan, K., D. Wu, J. C. An, and M. Prasant, “Comparing simulation tools and experimental testbeds for wireless mesh networks,” *2010 IEEE International Symposium on a World of Wireless Mobile and Multimedia Networks (WoWMoM)*, 1–9, Jun. 14–17, 2010.
 25. Osterlind, F. A. Dunkels, T. Voigt, N. Tsiftes, J. Eriksson, and N. Finne, “Sensornet checkpointing: Enabling repeatability in testbeds and realism in simulators,” *EWSN 2009*, Cork, Ireland, Feb. 2009.